HHS Public Access

Author manuscript

Hepatology. Author manuscript; available in PMC 2017 February 01.

Published in final edited form as:

Hepatology. 2016 February ; 63(2): 538–549. doi:10.1002/hep.28301.

Regulation of mechanosensitive biliary epithelial transport by the Epithelial Na^+ Channel, ENaC

Qin Li[1,5], **Charles Kresge**[5], **Abhijit Bugde**[3], **Michelle Lamphere**[2], **Jason Y. Park**[2,4,6], and **Andrew P. Feranchak**[5]

[1]Department of Physiology, Jianhan University School of Medicine, Wuhan, China

[2]Department of Pathology and Laboratory Medicine, Children's Health, Children's Medical Center, University of Texas Southwestern Medical Center, Dallas, TX

[3]Departments of Cell Biology, University of Texas Southwestern Medical Center, Dallas, TX

[4]Pathology, University of Texas Southwestern Medical Center, Dallas, TX

[5]Pediatrics, University of Texas Southwestern Medical Center, Dallas, TX

[6]Eugene McDermott Center for Human Growth and Development, University of Texas Southwestern Medical Center, Dallas, TX

Abstract

Intrahepatic biliary epithelial cells (BECs), also known as cholangiocytes, modulate the volume and composition of bile through the regulation of secretion and absorption. While mechanosensitive Cl^- efflux has been identified as an important secretory pathway, the counter absorptive pathways have not been identified. In other epithelial cells, the Epithelial Na^+ Channel (ENaC) has been identified as an important contributor to fluid absorption, however its expression and function in BECs has not been previously studied. Our studies revealed the presence of α,β, and γ ENaC subunits in human BECs and α, γ subunits in mouse BECs. In studies of confluent mouse BEC monolayers, ENaC contributes to the volume of surface fluid at the apical membrane during constitutive conditions. Further, functional studies utilizing whole cell patch clamp of single BECs demonstrated small constitutive Na^+ currents which increased significantly in response to fluid-flow or shear. The magnitude of Na^+ currents was proportional to the shear force, displayed inward rectification, a reversal potential of +40 mV (E_{Na+}= +60 mV), and were abolished with removal of extracellular Na^+ (NMDG) or in the presence of amiloride. Transfection with ENaCα siRNA significantly inhibited flow-stimulated Na^+ currents, while overexpression of the α subunit significantly increased currents. ENaC-mediated currents were positively regulated by proteases and negatively regulated by extracellular ATP. In conclusion, our studies represent the initial characterization of mechanosensitive Na^+ currents activated by flow in biliary epithelium. Understanding the role of mechanosensitive transport pathways may provide strategies to modulate the volume and composition of bile during cholestatic conditions.

Address correspondence to: Andrew Feranchak, M.D., UT Southwestern Medical Center, 5323 Harry Hines Boulevard, Dallas, TX 75390-9063, Telephone: 214-648-3118, FAX: 214-648-2673, drew.feranchak@utsouthwestern.edu.

INTRODUCTION

Biliary epithelial cells (BECs), also known as cholangiocytes, are the cells that form the intrahepatic bile ducts and contribute to the volume and composition of bile through the regulated transport of ions and water (1). Cl^- channels on the apical membrane provide the driving force for secretion (2) and are regulated by hormones acting on the basolateral membrane (such as secretin) and signals acting on the apical membrane such as fluid-flow/shear, and/or extracellular ATP (3). In fact, extracellular ATP acting on the apical membrane of BECs has emerged as a dominant pathway for the localized control of bile volume and composition (4-6). Released by the mechanical effects of shear force at the apical membrane of BECs, ATP is released into bile where it acts on purinergic (P2) receptors on the apical membrane to increase $[Ca^{2+}]_i$ and Cl^- secretion through Ca^{2+}-activated Cl^- channels (7, 8). Thus, mechanosensitive ATP release and activation of BEC P2 receptors is an important regulator of bile formation.

In contrast to the secretory pathways, the counter absorptive pathways in BECs have received little attention. In other epithelial cells, the Epithelial Na^+ Channel (ENaC) has been identified as an important contributor to fluid absorption. For example, in airway and renal epithelium constitutive and stimulated ENaC activity modifies the volume and composition of airway surface fluid and urine, respectively (9, 10). Located on the apical membrane of these epithelial cells, ENaC is a highly Na^+-selective, constitutively open channel comprised of three homologous subunits (α, β, γ)(11, 12). After transcription, the three subunits of ENaC traffic to the apical membrane and are activated by several pathways including proteases and the mechanical effects of shear force. The resulting increase in Na^+ influx drives water absorption at the apical membrane. Thus, ENaC is an important regulator of salt and water reabsorption in many types of epithelium and is essential for the maintenance of body salt and water homeostasis (12).

The balance between secretory and absorptive pathways in BECs must be finely regulated. This may be achieved through the local regulation of transport activity at the apical membrane of BECs. While extracellular ATP has emerged as an important mediator of biliary secretion, its potential counter role in the negative regulation of Na^+ and fluid absorption in BECs has not been previously explored. Furthermore, despite the importance of ENaC in multiple tissues, the presence of ENaC and its potential role in BEC transport is unknown. The aim of these studies therefore was to determine if ENaC is expressed in BECs, contributes to mechanosensitive Na^+ transport, and, if so, to identify the regulatory pathways involved.

METHODS

Cell models

Studies were performed in human Mz-Cha-1 cells (13) and in mouse small (MSC) and large (MLC) cholangiocytes isolated from normal mice (BALB/c) and immortalized by transfection with the SV40 large-T antigen gene as previously described (14) (15). For studies of apical surface liquid (ASL), MLC cells were cultured on collagen-coated semi-permeable transwell supports (Costar Corning, Acton, MA) for 7-10 days permitting the

development of highly polarized cells with a high transepithelial resistance (R_t > 1,000 Ω·cm^2).

Perfusion system

Shear was applied to cells in a parallel plate chamber (Warner Instruments, Hamden, CT) as described (8) . Flow was applied by a dual syringe pump (Harvard apparatus, Holliston, MA). The equation relating shear stress to volumetric flow rate through the chambers is given by $\tau_w = 6\mu Q/a^2 b$, where μ is the viscosity of the solution (poise), Q=flow rate (ml/sec), a=chamber height (cm), b=chamber width (cm).

Measurement of Na^+ currents

Membrane Na^+ currents were measured using whole-cell patch clamp techniques as previously reported (16). Cells on a cover slip were mounted in a chamber and whole cell currents measured with low Cl^- solutions to minimize the contribution of flow-stimulated Cl^- currents. Recordings were made with an Axopatch ID amplifier (Axon Instruments, Foster City, CA), and were digitized (1 kHz) and analyzed using pCLAMP version 10.0 programs (Axon Instruments) as previously described (3). Two voltage protocols were utilized: 1) holding potential −40 mV, steps to −100 mV and 0mv and +100mv at 5 second intervals (for real-time tracings), 2) holding potential −40 mV, with 400 ms steps from −100 mV to +100 mV in 10 mV increments. Current-voltage (I-V) relations were generated from the “step” protocols as indicated. Results are compared with control studies measured on the same day to minimize any effects of day-to-day variability and reported as current density (pA/pF) to normalize for differences in cell size. Details of the buffer solutions, voltage protocols, and data acquisition are provided in Supplemental materials.

Measurement of Apical Surface Liquid (ASL) height

The height of the fluid level at the apical membrane of confluent mouse cholangiocyte monolayers was performed according to a modified technique previously described in airway epithelial monolayers (17). Briefly, confluent MLC cells on 24mm collagen-coated transwell permeable membranes with a transepithelial resistance > 1,000 Ω·cm^2 were washed with PBS and labeled with Calcein-AM. The transwell was then placed on the surface of a glass-bottomed MatTek 35mm dish over a serosal reservoir and 80 μl of Dextran-Red (10 kDa, 2 mg/ml, Molecular Probes) in PBS was added to the apical chamber. Transwells were then mounted on a Zeiss LSM510 Confocal microscope and images acquired using a Zeiss 40x/0.8 water immersion lens. All images were analyzed with ImageJ (http://rsb.info.nih.gov), as previously described (18).

Detection of ENaC

PCR products representing the α, β, and γ subunits of ENaC were detected utilizing specific primers (Supplemental Table 1) and oligo(dt) primer and Superscript RNase H-reverse transcriptase (Invitrogen, Carlsbad, CA). ENaCα protein was detected by Western blot utilizing primary anti-human ENaCα, which recognizes an extracellular region contained in both the full-length and cleaved protein, at 1:200 (Alomone labs, Israel), followed by

incubation with peroxidase-conjugated goat anti-rabbit antibody, dilution 1:10,000 (Jackson ImmunoResearch Laboratories Inc., PA).

Immunofluorescence

Localization of ENaCα protein was performed in confluent MLC monolayers utilizing anti-ENaCα antibody (Alomone labs) and then Dylight 488 conjugated donkey anti-rabbit antibody (Jackson, 1:600) and counter-labeled with DAPI and Alexa Fluor 555 phalloidin. The slides were imaged using the Leica TCS SP5 confocal microscope with custom software (Leica Micro-systems, CMS GMBH and LAS AF).

Immunohistochemistry

Immunohistochemistry was performed on paraffin sections of mouse liver to evaluate localization of ENaCα. Wild-type C57BL/6 mouse liver sections were fixed in10% neutral buffered formalin and paraffin embedded. Further processing steps were performed on the Dako Omnis automated immunohistochemistry platform (Glostrup, Denmark). Sections were incubated with mouse polyclonal ENaCα antibody at a 1:800 dilution (#PA1-920A, Thermo Fisher Scientific, Waltham, MA). Endogenous peroxidase blocking was performed and then followed by incubation with a secondary HRP antibody mixture of goat anti-rabbit and goat anti-mouse for 20 minutes.

Overexpression of ENaC subunits

Full-length ENaC α, β, γ, channel subunits were kind gift from Chou-Long Huang (UT Southwestern, Dallas, TX) (19) and were amplified and purified by using Macherey-Nagel NucleoBond® Xtra Midi / Maxi. Cells at ~70% confluency in 35 mm dishes were treated with 4μg of total plasmid cDNA encoding α, β, γ ENaC and GFP using the lipofectamin 2000 (Invitrogen) per the manufacturer's recommendations. GFP-labeled cells were used for patch clamp analysis or extracted for protein analysis 48 hours after transfection.

ENaC silencing

ENaCα was suppressed by specific ENaCα siRNA (NM_001159576). siRNAs were designed and synthesized by IDT (5'- AGC UUU GAC AAG GAA CUU UCC UAA G -3'; 3'-CCU CGA AAC UGU UCC UUG AAA GGA UUC-5') and control sequence (5'-CGU UAA UCG CGU AUA AUA CGC GUA T -3', 3'-AUA CGC GUA UUA UAC GCG AUU AAC GAC -5'). Cells were transfected using Lipofectamine RNAiMAX reagent from Invitrogen. Block-it™ Fluorescent Oligo (Invitrogen) was used to optimize transfection conditions and for selection of transfected cells for whole-cell patch clamp current recording. Whole cell patch clamp experiments were done 48 hours after transfection.

Reagents and Statistics

Detailed descriptions of the reagents, buffer solutions, experimental protocols, and statistical analysis are provided in Supplemental Materials.

RESULTS

Detection of ENaC in biliary epithelium

Utilizing selective primers (Supplementary Table 1) for the specific ENaC subunits (α, β, and γ), PCR products of the predicted size for ENaCα were detected in all human and mouse biliary cells (Figure 1A). Additionally, PCR products of the predicted size for β and γ subunits were detected in human biliary cells, while γ was found in mouse biliary cells. PCR products for the β subunit were not found in mouse BECs. Western blot analysis, utilizing specific anti-ENaCα antibody, detected a predicted protein band ~90 kDa in all biliary cells (Figure 3A). Immunostaining of polarized mouse monolayers revealed ENaCα on the apical plasma membrane (Figure 1B). Immunohistochemistry of whole mouse liver sections revealed ENaCα in the apical membrane of intrahepatic ducts and gallbladder (Figure 1C).

Mechanosensitive Na^+ currents in BECs

Previously, we have shown that fluid-flow activates small cation currents and large anion currents in BECs (20). While the anion currents are predominantly due to the Ca^{2+}-activated Cl^- channel, TMEM16A (7), the identity of the flow-stimulated cation currents is unknown. To isolate and evaluate the smaller cation currents, Cl^- was removed from the bath and pipette solutions. Under static (no flow) conditions small constitutive currents were measured (Figure 2). Exposure to flow (shear of 0.12 dyne/cm^2) rapidly increased endogenous membrane currents in 87% of human biliary cells (n=96) and 92% of mouse cells (n=15). The currents reached a maximum within 90 seconds and then decreased with continued flow exposure. Currents displayed inward rectification, a reversal potential of +40 mV (E_{Na+}= +60 mV), and time-dependent inactivation at membrane potentials >60 mV. Flow-stimulated currents were abolished when Na^+ was replaced with equimolar concentration of NMDG, confirming Na^+ as the predominant charge carrier. The magnitude of Na^+ currents was proportional to the shear force, reaching a maximum at a shear of 0.24 dyne/cm^2 and a $K_{1/2\ max}$ of 0.06 dyne/cm^2 (Figure 2C and Supplemental Figure 2). In the presence of the ENaC inhibitor amiloride currents were inhibited by 67± 4.5%. Thus, the biophysical and pharmacologic properties of the endogenous flow-stimulated Na^+ currents in BECs are consistent with those previously reported for ENaC in other epithelium (9, 10, 21).

Functional role of ENaCα in mediating Na^+ currents

It has previously been shown that the α subunit of ENaC is a key regulator of flow-activated Na^+ currents (22). To identify the molecular basis of the flow-stimulated Na^+ currents in human BECs and determine if the α subunit plays a role in channel activation, whole-cell currents were measured in cells transfected with antisense oligonucleotides targeting α-hENaC and compared to non-transfected cells (control) and cells transfected with non-targeting siRNA (mock) (Figure 3). First, transfection with ENaCα siRNA decreased mRNA by 47± 2% and protein levels by 48 ± 3% compared to mock transfected cells. Next, whole cell patch clamp studies were performed to determine the functional effect of the decrease in ENaCα expression (Figure 3). In control or mock transfected cells, small constitutive Na^+ currents were observed. Exposure to flow resulted in a significant increase in the magnitude of Na^+ currents which again were inhibited by the ENaC inhibitor,

amiloride. Transfection with ENaCα siRNA had no significant effect on constitutive currents, but significantly decreased the magnitude of flow-stimulated Na^+ currents. Thus, the ENaC α subunit is a significant contributor to flow-mediated Na^+ currents in BECs.

Functional effects of overexpression of ENaC subunits on flow-stimulated currents

To further characterize the role of the ENaCα subunit in flow-activated Na^+ currents, ENaCα was overexpressed in Mz-Cha-1 cells (Figure 4). Of note, GFP was co-transfected as a marker of transfection efficiency and cell selection for whole cell patch clamp. First, overexpression of ENaCα increased protein expression by 200 ± 5%. Second, in ENaCα overexpressing cells, the magnitude of flow-stimulated Na^+ currents increased by 73 ± 8% compared to mock transfected. Currents displayed time-dependent inactivation, reversal at +40 mv, and were inhibited by amiloride. While previous studies in *Xenopus* oocytes demonstrated that the expression of the ENaCα subunit alone is sufficient to induce amiloride-sensitive Na^+ currents, co-expression of the β and γ subunits resulted in Na^+ currents of greater magnitude (23). To determine if over expression of these subunits similarly effects Na^+ currents in BECs, the three ENaC subunits, α, β, and γ, were simultaneously overexpressed in Mz-Cha-1 cells and whole cell currents were measured. Overexpression of the three subunits did not affect the magnitude of Na^+ currents measured under basal (constitutive) conditions, but significantly increased the magnitude of Na^+ currents in response to flow compared to mock transfected or control cells. However, the magnitude of the flow-stimulated currents was not significantly different between cells overexpressing the α subunit alone versus those overexpressing all three subunits together. Overall, the results demonstrate that the α subunit appears to be the critical subunit in this response, as there was no further increase in the magnitude of Na^+ currents when β, and γ subunits were also co-expressed.

Regulation of ENaC by proteases

One mechanism by which ENaC is activated involves proteolytic cleavage of ENaC subunits by membrane-associated or soluble serine proteases (24). To determine if ENaC in BECs is activated by proteases, whole cell patch clamp studies were performed to measure Na^+ currents in the presence or absence of trypsin (Figure 5). During basal conditions characteristic small constitutive Na^+ currents were measured. In the absence of flow, application of trypsin to the bath increased the magnitude of Na^+ currents significantly. Currents reached a maximum within 108 ± 5 seconds of trypsin exposure, and displayed biophysical properties identical to flow-activated Na^+ currents. After current activation by trypsin, no additional increase in the magnitude of Na^+ currents was observed with subsequent flow exposure. Likewise, following flow exposure the addition of trypsin did not increase currents further (Supplemental Figure 3). Thus, these distinct stimuli (trypsin and flow) appear to be acting on the same Na^+ channel (i.e. ENaC). Next, to determine if endogenous proteases contribute to ENaC activation in response to flow, whole cell currents were measured in the presence or absence of trypsin inhibitor. In the presence of trypsin inhibitor, exposure to flow failed to activate currents (Figure 5B). When trypsin inhibitor was removed from the perfusate, activation of Na^+ currents occurred and exhibited characteristic properties consistent with ENaC activation. Lastly, the effects of trypsin on ENaCα cleavage was determined by evaluating ENaC subunit expression and size by

Western blots. These results demonstrate that trypsin directly cleaves the α subunit as demonstrated by the appearance of a secondary band at ~37kD in addition to the full length band at ~90 kD (Figure 5C). The cleaved fragment was observed after 2 minutes of incubation with trypsin and image intensity reached a maximum by 5 minutes. Together the studies are consistent with a model in which trypsin opens the channel through cleavage of the α subunit and demonstrate that protease activity is necessary for flow-stimulated ENaC activation in BECs.

ENaC contributes to the volume of fluid at the apical membrane

To determine the potential role of ENaC in modulating fluid volume, studies were performed to measure the height of the surface fluid at the apical membrane of confluent mouse cholangiocytes. As shown in Figure 7, addition of amiloride to inhibit ENaC significantly increased the height of ASL. This is consistent with ENaC contributing to basal Na^+ and fluid absorption. In separate studies, addition of ATP to the apical membrane also resulted in significant increases in ASL. The cumulative data reveals that ATP has similar effects on ASL height as amiloride. Addition of both amiloride and ATP together resulted in an increase in ASL height which was significantly greater than amiloride alone. Together these results demonstrate that ENaC contributes to the volume of fluid at the apical membrane during constitutive conditions.

Negative regulation of ENaC by extracellular ATP

While we have previously shown that ATP activates Ca^{2+}-activated Cl^- channels and fluid secretion from BECs, the possibility that ATP may also directly inhibit ENaC exists. To determine if extracellular ATP directly inhibits ENaC activity, whole cell patch clamp studies were performed. In control cells, fluid-flow activated characteristic Na^+ currents; however addition of ATP to the perfusate rapidly inhibited currents. The inhibitory effect of ATP was reversible and currents could be re-activated by flow when ATP was removed. Apyrase, to hydrolyze ATP, had opposite effects on flow-activated Na^+ currents and significantly increased the magnitude of flow-stimulated Na^+ currents compared to flow-stimulated currents without apyrase. Together these studies demonstrate that ATP negatively regulates ENaC channel activity in response to flow.

DISCUSSION

The present studies provide evidence that ENaC is present in BECs and contributes to constitutive and flow-stimulated Na^+ absorption. To our knowledge these represent the first functional studies of ENaC in BECs. ENaC is a member of the Deg/ENaC ion channel superfamily that contain a functionally diverse array of channels, but all share a common structure consisting of subunits that have two transmembrane spanning regions, a large extracellular domain, and two short cytosolic tails(25). In native epithelia, ENaC is composed of three homologous but distinct subunits: α, β, and γ; though expression of the α subunit alone has been associated with Na^+ currents in some models (11, 26). Our studies also support an essential role of the α subunit in ENaC-mediated Na^+ currents in BECs. First, transfection with siRNA targeting the α subunit significantly inhibited the flow-stimulated Na^+ currents in endogenously expressing human BECs. Second, overexpression

of the α subunit in human BECs increased the magnitude of flow-stimulated currents, while the additional overexpression of the other subunits β and γ, did not result in any further increase in the magnitude of flow-stimulated currents. Of note, we did not find PCR products for the β subunit of ENaC in any of the mouse models (MSC, MLC). However, this is consistent with previous findings in whole mouse liver where β ENaC was not detected(27).

First, the mechanism by which BEC ENaC activity is modulated by proteases *in vivo* is unknown. It is thought that regulation of ENaC by proteases occurs through protease-dependent cleavage of one or more of the extracellular loops of the subunits at specific consensus cleavage sites (24, 28) . In our studies, addition of trypsin during basal conditions resulted in cleavage of the α subunit and activated Na^+ currents. Furthermore, in separate studies, flow failed to activate currents in the presence of trypsin inhibitor, suggesting that flow mediates current activation through endogenous proteases in BECs. Interestingly, proteases are found in bile (29, 30). This is intriguing and suggests that in the presence of flow, proteases may be liberated from the apical plasma membrane of BECs, thereby increasing the concentration of free proteases in bile and subsequently modulating apical membrane transport. However, the expression, function, and characterization of membrane-associated, or soluble, proteases in BECs or bile, respectively, are unknown.

Second, the mechanism by which ATP exerts inhibitory effects on ENaC is unknown. In the current studies, we have shown that ATP inhibits ENaC currents in single cells and inhibits fluid reabsorption in cholangiocyte monolayers. These findings are similar to findings in renal epithelium, where ATP inhibits ENaC in the collecting duct and prevents Na^+ reabsorption. ATP activates P2Y2 receptors, which are G-protein coupled receptors that increases PLC activity via Gq/11, resulting in PI (4,5)P2 hydrolysis and generation of inositol 1,4,5-triphosphate (IP3). In previous studies of renal epithelial cells, the loss of PI(4,5)P2 was thought to result in ENaC inhibition (31). Interestingly, P2Y2 is the predominant P2Y receptor in BECs and activation is linked to PLC activity and IP3 generation resulting in release of Ca^{2+} from intracellular stores and activation of membrane Ca^{2+}-activated Cl^- channels (4)(7) . Thus, the P2Y2 – PLC – IP3 pathway may simultaneously activate the secretory pathway and inhibit the absorptive pathway.

We have previously shown that fluid flow is a stimulus for ATP release and activation of TMEM16A, a Ca^{2+}-activated Cl^- channel at the apical membrane of cholangiocytes(8, 15, 20). Thus, the same stimulus (i.e. fluid-flow) which activates ENaC also stimulates ATP release and Cl^- secretion. It is initially surprising that fluid-flow activates both Cl^-channels and Na^+ channels, however our hypothesis is that shear initially and transiently increases Na^+ currents via direct proteolytic cleavage of ENaCα by cell surface or soluble proteases (32, 33); while at sustained shear, released ATP inhibits ENaC-mediated Na^+ currents. Thus, ATP is an important regulator of bile formation by activating secretory and concurrently inhibiting absorptive pathways (Figure 7), a hypothesis consistent with findings in other model systems where ductular secretion is dependent on extracellular ATP (5, 6). As there is always some ATP in bile (34, 35), the balance between secretory and absorptive pathways determines the constitutive volume during basal or resting conditions.

Lastly, the role of ENaC during cholestatic liver disease, associated with a decrease in bile flow, is unknown. Lack of the mechanical flow stimulus at the apical membrane would cause a decrease in ATP release into the duct lumen resulting in i) a decrease in Cl^- secretion, and ii) an increase in Na^+ and fluid reabsorption. For example, the cholestatic liver disease associated with cystic fibrosis (CF) is associated with a decrease in bile flow, thickened inspissated secretions, and bile duct plugging in some patients (36). In fact, CF is associated with increased ENaC activity and hyperabsorption of Na^+ in some epithelial models (37). The role of ENaC in cholestatic liver diseases associated with decreases in bile flow requires further study. Targeting the elements of the mechanosensitive signaling pathway including ATP release, P2 receptors, and/or ENaC, therefore, may provide new and innovative strategies to modulate the volume and composition of bile during cholestatic liver disease.

Supplementary Material

Refer to Web version on PubMed Central for supplementary material.

ACKNOWLEDGMENTS

The authors wish to thank Chou-Long Huang, UT Southwestern, Dallas, TX, for kindly providing the constructs for full-length ENaC subunits. This study was supported by the Children's Medical Center Foundation, the Cystic Fibrosis Foundation, and the National Institute of Diabetes, Digestive and Kidney Diseases (NIDDK) of the National Institute of Health grant R01DK078587 (APF).

Reference List

1. Fitz, JG. Cellular mechanisms of bile secretion. In: Zakim, D.; Boyer, TD., editors. Hepatology. 3. W.B. Saunders Company; Philadelphia: 1996. p. 362-376.
2. Fitz JG, Basavappa S, McGill J, Melhus O, Cohn JA. Regulation of membrane chloride currents in rat bile duct epithelial cells. J Clin Invest. 1993; 91:319–328. [PubMed: 7678606]
3. Roman RM, Feranchak AP, Salter KD, Wang Y, Fitz JG. Endogenous ATP regulates Cl^- secretion in cultured human and rat biliary epithelial cells. Am J Physiol. 1999; 276:G1391–G1400. [PubMed: 10362642]
4. Dutta AK, Woo K, Doctor RB, Fitz JG, Feranchak AP. Extracellular nucleotides stimulate Cl- currents in biliary epithelia through receptor-mediated IP3 and Ca2+ release. Am J Physiol Gastrointest Liver Physiol. 2008; 295:G1004–G1015. [PubMed: 18787062]
5. Fiorotto R, Spirli C, Fabris L, Cadamuro M, Okolicsanyi L, Strazzabosco M. Ursodeoxycholic acid stimulates cholangiocyte fluid secretion in mice via CFTR-dependent ATP secretion. Gastroenterology. Nov; 2007 133(5):1603–1613. [PubMed: 17983806]
6. Minagawa N, Nagata J, Shibao K, Masyuk AI, Gomes DA, Rodrigues MA, et al. Cyclic AMP regulates bicarbonate secretion in cholangiocytes through release of ATP into bile. Gastroenterology. Nov; 2007 133(5):1592–1602. [PubMed: 17916355]
7. Dutta AK, Khimji AK, Kresge C, Bugde A, Dougherty M, Esser V, et al. Identification and Functional Characterization of TMEM16A, a Ca2+-activated Cl-Channel Activated by Extracellular Nucleotides, in Biliary Epithelium. J Biol Chem. Jan 7; 2011 286(1):766–776. [PubMed: 21041307]
8. Woo K, Dutta AK, Patel V, Kresge C, Feranchak AP. Fluid flow induces mechanosensitive ATP release, calcium signalling and Cl-transport in biliary epithelial cells through a PKCzeta-dependent pathway. J Physiol. Jun 1; 2008 586(Pt 11):2779–2798. [PubMed: 18388137]
9. Myerburg MM, Harvey PR, Heidrich EM, Pilewski JM. Butterworth MB. Acute regulation of the epithelial sodium channel in airway epithelia by proteases and trafficking. Am J Respir Cell Mol Biol. Dec; 2010 43(6):712–719. [PubMed: 20097829]

10. Satlin LM, Sheng S, Woda CB, Kleyman TR. Epithelial Na(+) channels are regulated by flow. Am J Physiol Renal Physiol. Jun; 2001 280(6):F1010–F1018. [PubMed: 11352841]
11. Canessa CM, Schild L, Buell G, Thorens B, Gautschi I, Horisberger JD, et al. Amiloride-sensitive epithelial Na+ channel is made of three homologous subunits. Nature. Feb 3; 1994 367(6462): 463–467. [PubMed: 8107805]
12. Garty H. Molecular properties of epithelial, amiloride-blockable Na+ channels. FASEB J. May; 1994 8(8):522–528. [PubMed: 8181670]
13. Knuth A, Gabbert H, Dippold W, Klein O, Sachsse W, Bitter-Suermann D, et al. Biliary Adenocarcinoma. Characterization of three new human tumor cell lines. J Hept. 1985; 1:579–596.
14. Ueno Y, Alpini G, Yahagi K, Kanno N, Moritoki Y, Fukushima K, et al. Evaluation of differential gene expression by microarray analysis in small and large cholangiocytes isolated from normal mice. Liver Int. Dec; 2003 23(6):449–459. [PubMed: 14986819]
15. Woo K, Sathe M, Kresge C, Esser V, Ueno Y, Venter J, et al. Adenosine triphosphate release and purinergic (P2) receptor-mediated secretion in small and large mouse cholangiocytes. Hepatology. Nov; 2010 52(5):1819–1828. [PubMed: 20827720]
16. Feranchak AP, Berl T, Capasso J, Wojtaszek PA, Han J, Fitz JG. p38 MAP kinase modulates liver cell volume through inhibition of membrane Na+ permeability. J Clin Invest. Nov; 2001 108(10): 1495–1504. [PubMed: 11714741]
17. Tarran R, Trout L, Donaldson SH, Boucher RC. Soluble mediators, not cilia, determine airway surface liquid volume in normal and cystic fibrosis superficial airway epithelia. J Gen Physiol. May; 2006 127(5):591–604. [PubMed: 16636206]
18. Tarran R, Button B, Boucher RC. Regulation of normal and cystic fibrosis airway surface liquid volume by phasic shear stress. Annu Rev Physiol. 2006; 68:543–561. [PubMed: 16460283]
19. Xu BE, Stippec S, Chu PY, Lazrak A, Li XJ, Lee BH, et al. WNK1 activates SGK1 to regulate the epithelial sodium channel. Proc Natl Acad Sci U S A. Jul 19; 2005 102(29):10315–10320. [PubMed: 16006511]
20. Dutta AK, Woo K, Khimji AK, Kresge C, Feranchak AP. Mechanosensitive Cl-secretion in biliary epithelium mediated through TMEM16A. Am J Physiol Gastrointest Liver Physiol. Jan 1; 2013 304(1):G87–G98. [PubMed: 23104560]
21. Lazrak A, Samanta A, Matalon S. Biophysical properties and molecular characterization of amiloride-sensitive sodium channels in A549 cells. Am J Physiol Lung Cell Mol Physiol. Apr; 2000 278(4):L848–L857. [PubMed: 10749763]
22. Jain L, Chen XJ, Malik B, Al-Khalili O, Eaton DC. Antisense oligonucleotides against the alpha-subunit of ENaC decrease lung epithelial cation-channel activity. Am J Physiol. Jun; 1999 276(6 Pt 1):L1046–L1051. [PubMed: 10362730]
23. Canessa CM, Horisberger JD, Rossier BC. Epithelial sodium channel related to proteins involved in neurodegeneration. Nature. Feb 4; 1993 361(6411):467–470. [PubMed: 8381523]
24. Vallet V, Chraibi A, Gaeggeler HP, Horisberger JD, Rossier BC. An epithelial serine protease activates the amiloride-sensitive sodium channel. Nature. Oct 9; 1997 389(6651):607–610. [PubMed: 9335501]
25. Benos DJ, Stanton BA. Functional domains within the degenerin/epithelial sodium channel (Deg/ENaC) superfamily of ion channels. J Physiol. Nov 1; 1999 520(Pt 3):631–644. [PubMed: 10545131]
26. Lingueglia E, Renard S, Waldmann R, Voilley N, Champigny G, Plass H, et al. Different homologous subunits of the amiloride-sensitive Na+ channel are differently regulated by aldosterone. J Biol Chem. May; 1994 13(269):19–13736.
27. Ahn YJ, Brooker DR, Kosari F, Harte BJ, Li J, Mackler SA, et al. Cloning and functional expression of the mouse epithelial sodium channel. Am J Physiol. Jul; 1999 277(1 Pt 2):F121–F129. [PubMed: 10409305]
28. Hughey RP, Mueller GM, Bruns JB, Kinlough CL, Poland PA, Harkleroad KL, et al. Maturation of the epithelial Na+ channel involves proteolytic processing of the alpha- and gamma-subunits. J Biol Chem. Sep; 2003 26(278):39–37073.

29. Musil LS, Baenziger JU. Proteolytic processing of rat liver membrane secretory component. Cleavage activity is localized to bile canalicular membranes. J Biol Chem. Oct; 1988 25(263):30–15799.

30. Packialakshmi B, Liyanage R, Rasaputra KS, Lay JO Jr. Rath NC. Isolation and characterization of chicken bile matrix metalloproteinase. Poult Sci. Jun; 2014 93(6):1495–1502. [PubMed: 24879699]

31. Yue G, Malik B, Yue G, Eaton DC. Phosphatidylinositol 4,5-bisphosphate (PIP2) stimulates epithelial sodium channel activity in A6 cells. J Biol Chem. Apr; 2002 5(277):14–11965.

32. Svenningsen P, Friis UG, Bistrup C, Buhl KB, Jensen BL, Skott O. Physiological regulation of epithelial sodium channel by proteolysis. Curr Opin Nephrol Hypertens. Sep; 2011 20(5):529–533. [PubMed: 21670672]

33. Rossier BC, Stutts MJ. Activation of the epithelial sodium channel (ENaC) by serine proteases. Annu Rev Physiol. 2009; 71:361–379. [PubMed: 18928407]

34. Chari RS, Schutz SM, Haebig JA, Shimokura GH, Cotton PB, Fitz JG, et al. Adenosine nucleotides in bile. Am J Physiol. 1996; 270:G246–G252. [PubMed: 8779965]

35. Nathanson MH, Burgstahler AD, Masyuk A, LaRusso NF. Stimulation of ATP secretion in the liver by therapeutic bile acids. Biochem J. Aug 15; 2001 358(Pt 1):1–5. [PubMed: 11485545]

36. Feranchak AP, Sokol RJ. Cholangiocyte biology and cystic fibrosis liver disease. Sem Liv Disease. 2001; 21:471–488.

37. Boucher RC, Stutts MJ, Knowles MR, Cantley L, Gatzy JT. Na+ transport in cystic fibrosis respiratory epithelia. Abnormal basal rate and response to adenylate cyclase activation. J Clin Invest. Nov; 1986 78(5):1245–1252. [PubMed: 3771796]

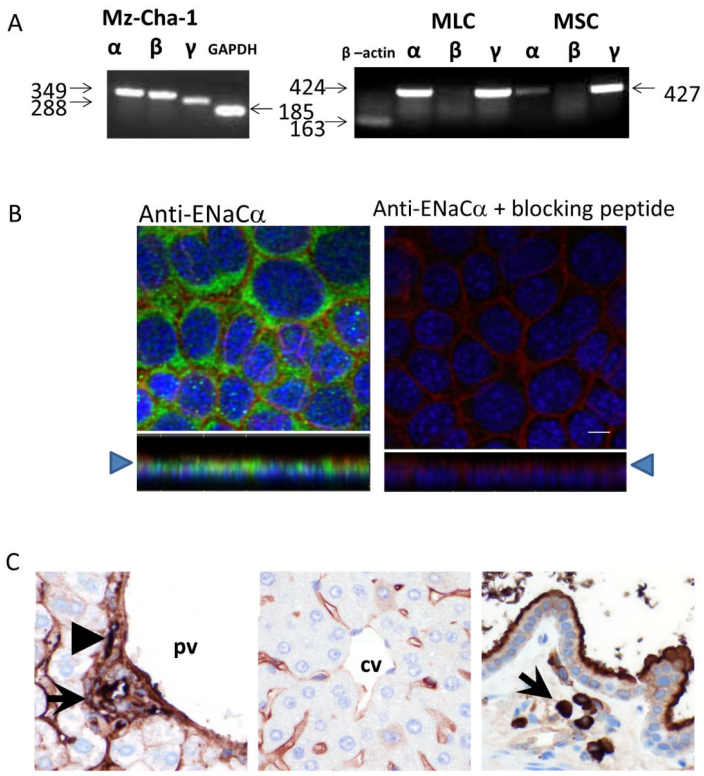

Figure 1. Expression and localization of ENaC in biliary epithelium

A. RT-PCR. Species specific ENaC subunit primers were used to detect ENaC subunits in all models. In human biliary Mz-Cha-1 cells, ENaC α, β, and γ were detected (band sizes of 349, 349, and 288 respectively). In mouse large cholangiocytes (MLC, left panel) and mouse small cholangiocytes (MSC, right panel) ENaCα and γ (band sizes of 424 and 427, respectively) were detected. B. Membrane localization of ENaCα protein in polarized MLC monolayers. Staining with Alexa Fluor 555 phalloidin (red), to label the cell membrane, anti-ENaCα antibody (green), and DAPI (blue), demonstrates ENaCα protein in the apical plasma membrane, right panel (x-z plane shown below each image, arrow head indicates apical membrane). Control preparations (without primary antibody), right panel. Scale bar =10μm. C. Localization of ENaCα in mouse whole liver sections. Left panel, ENaCα was expressed on the apical membrane of intrahepatic bile ducts (arrow) and hepatic artery (arrow head). Middle panel, ENaCα is also detected in hepatic sinusoids lined by endothelial cells, while the portal vein (pv) and central vein (cv), have weaker expression. Right panel, the gallbladder shows strong staining in both the apical surface of the epithelial cells as well as macrophages in the lamina propria (arrow). All images at 400x magnification.

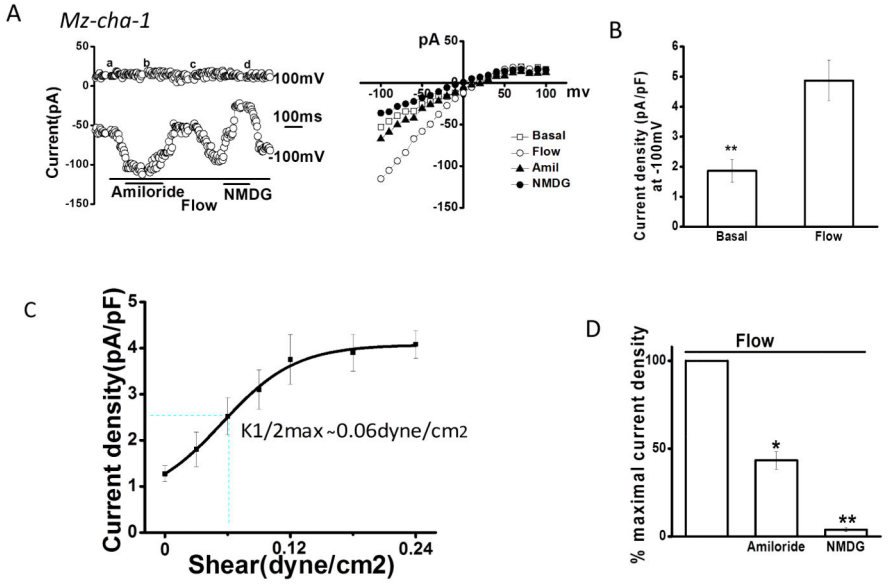

Figure 2. Fluid-flow/shear activates Na^+ currents

Whole-cell currents were measured during basal conditions and during exposure to flow of isotonic low Cl^- extracellular buffer (Methods). A. Representative whole-cell recording of Mz-Cha-1 cell. Currents measured at −100 mV and at 100 mV are shown. Flow exposure (shear of 0. 24 dyne/cm^2) is indicated by the bar. Addition of amiloride (100 μM) or replacement of Na^+ with NMDG is indicated by the lower bars. The I–V plot shown in the right panel was generated from the voltage-step protocol (Methods) and currents during basal (-□-) and flow-stimulated (-○-) conditions in the presence of amiloride (-△-) and with replacement of Na^+ with NMDG (-●-) are shown. B. Cumulative data demonstrating maximal flow-stimulated current density in Mz-Cha-1 cells. Bars represent maximal current density (pA/pF) measured at −100 mV; n = 50 each, *p<0.01. C. Shear-dependent response curve for Na^+ currents. Data were plotted from maximum current density (pA/pF) measured at −100 mV in response to different flow rates. Each point represents mean ± S.E. (n= 4-15) fit to the Hill equation. Calculated $K_{1/2}$ max = 0.06 dyne/cm^2. D. Cumulative data demonstrating % maximal flow-stimulated Na^+ currents in the presence of amiloride (n=56) left panel; or after replacement of Na^+ with NMDG (n=12), right panel. Values represent % of maximal current density measured at −100 mV. *p<0.05 and **p<0.01.

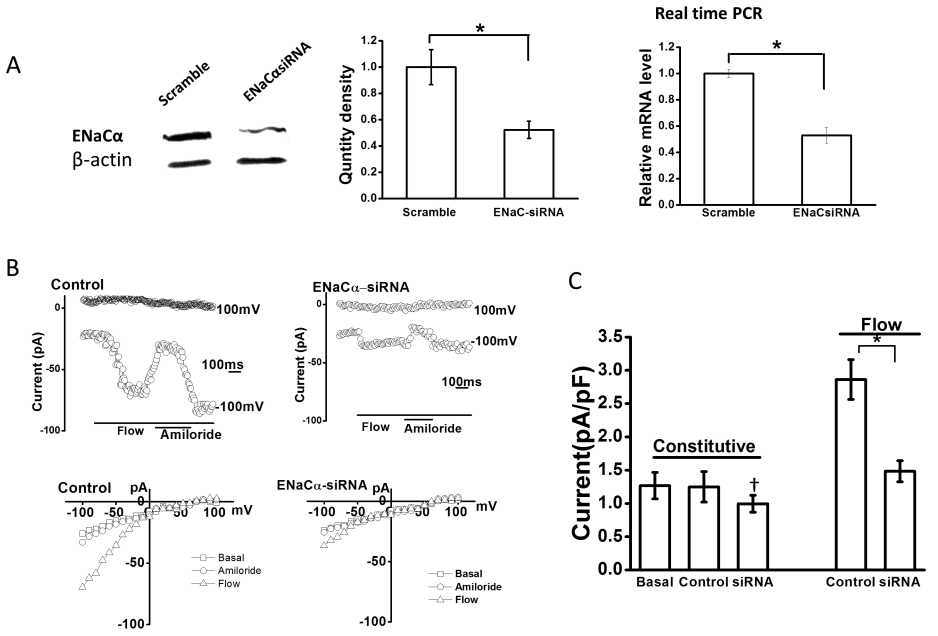

Figure 3. Role of ENaCα subunit in flow-stimulated Na^+ currents

A. Representative Western blot (left panel), and cumulative data (middle) demonstrating ENaCα protein levels in cells transfected with non-targeting siRNA (scramble), and cells transfected with ENaCα siRNA. β-actin used as loading control (**p* < 0.05 *versus scramble* levels). Right panel, relative mRNA levels, assessed by real-time PCR, in cells transfected with non-targeting siRNA (scramble) and cells transfected with ENaCα siRNA (**p* < 0.05 *versus scramble* levels). B. Representative whole-cell current recordings from Mz-Cha-1 cells transfected with non-targeting siRNA (control), left panel, or with ENaCα siRNA, right panel, under basal and flow-stimulated conditions. Flow exposure (0.24 dyne/cm^2) and amiloride application indicated by bars below the current trace. Currents measured at −100 mV and at +100 mV are shown. The *I–V* plots shown below the traces were generated from the step protocol (Methods) and show currents during basal (-□-), flow-stimulated (-△-) conditions, and flow-stimulated in the presence of amiloride (-□-). C. Cumulative data demonstrating maximal current density (pA/pF) measured at −100 mV under basal (constitutive) conditions and in response to flow in cells transfected with non-targeting siRNA (control), or cells transfected with ENaCα siRNA (bars represent mean ± S.E.; n=5 each). **p*<0.05 *versus* control; **p=n.s.

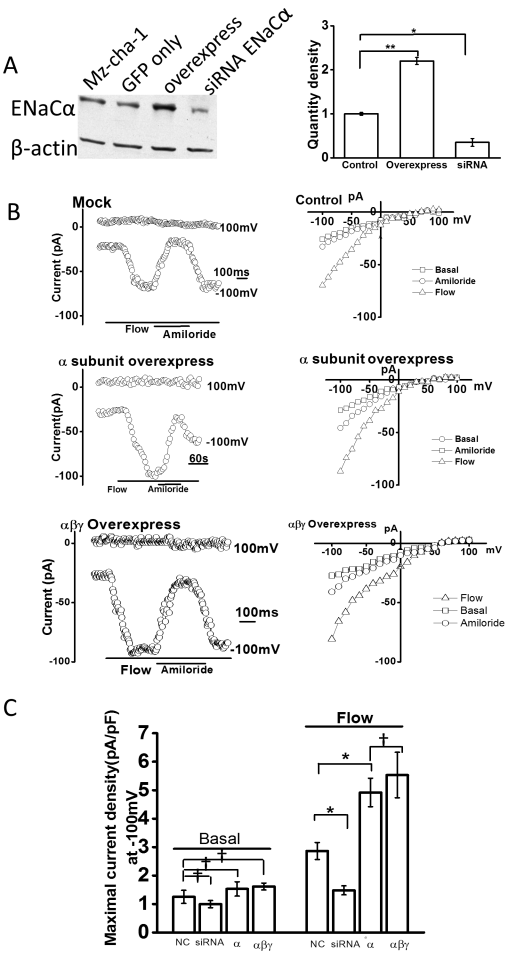

Figure 4. Functional effects of overexpression of ENaC subunits on flow-stimulated Na^+ currents

A. Representative Western blot (left panel) and cumulative data (right panel) demonstrating relative change in ENaCα protein level in control Mz-Cha-1 cells, cells transfected with non-targeting siRNA (mock), ENaCα siRNA, ENaC α subunit (overexpression), and GFP alone. β-actin used as loading control. *p<0.05 and **p<0.01 versus control protein levels. B. Representative whole cell recordings from cells transfected with non-targeting siRNA (mock, top panel), ENaCα (overexpression, middle) or ENaC α, β, and γ together (bottom panel). Flow exposure, and addition of amiloride, indicated by lines at bottom. IV plots for each transfection condition shown on the right and demonstrate currents during basal (-□-), flow (-△-), and flow in presence of amiloride (-□-) conditions. C. Cumulative data demonstrating maximal current density (pA/pF) measured at −100 mV in response to flow in cells transfected with non-targeting siRNA (non-coding, nc), ENaCα siRNA, ENaC α subunit (overexpression), and ENaCα, β, and γ subunits together under basal conditions and in response to flow (shear of 0.24 dyne/cm^2). Bars represent mean ± S.E., n=5 – 10 each, *p<0.05 *versus* mock (nc), †p= n.s.

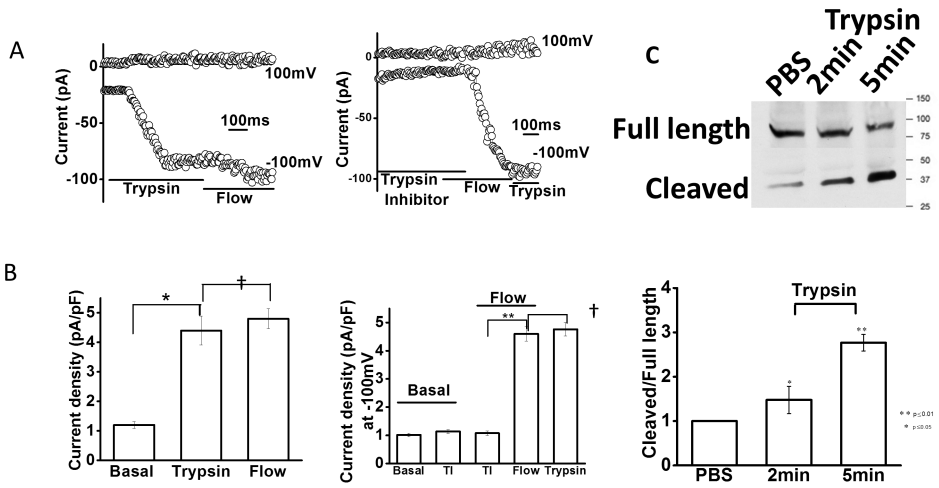

Figure 5. Modulation of Na^+ currents by proteases

Representative whole-cell recordings of Mz-Cha-1 cells in the presence or absence of trypsin or trypsin inhibitor. A. Currents in response to trypsin (10 μM) followed by flow (shear 0.24 dyne/cm^2; top), and cumulative data demonstrating maximal current density measured at −100 mV during this sequential exposure (bottom). B. Top panel, currents in response to flow (shear =0.24 dyne/cm^2) in the presence of trypsin inhibitor (25 μg/ml). Bottom panel, cumulative data demonstrating maximal current density at −100 mV under basal conditions, in response to trypsin inhibitor (TI), trypsin inhibitor (TI) and flow together, flow, and trypsin (20 μM); n=4 - 5 each, **p<0.05; †p=n.s. C. Western blot analysis. Incubation with trypsin (10 μM) resulted in appearance of secondary band at ~37kD in addition to the full length band at ~90kD by 2 minutes (top panel); cumulative data represents relative band density of ratio of cleaved to full-length fragment after incubation with trypsin for 2 or 5 minutes, control cells treated with PBS (bottom panel); n=4-5 trials each, *p<0.05, **p<0.01 versus control.

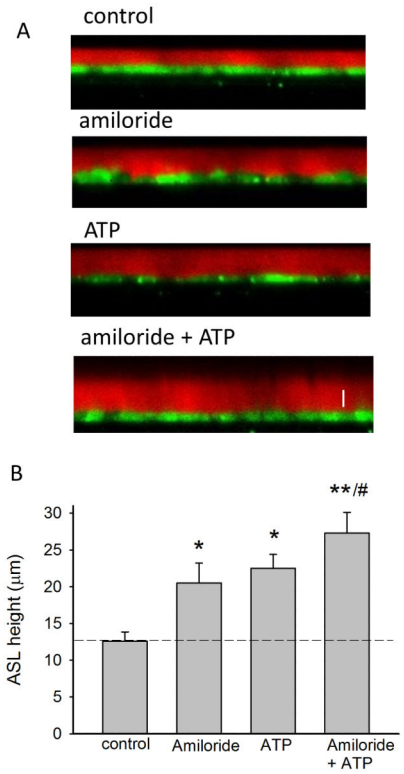

Figure 6. Apical Surface Liquid (ASL) height in mouse cholangiocyte monolayers

A. Representative X-Z confocal images of confluent polarized mouse cholangiocyte monolayers (green) after apical addition of Dextran-Red (red) to the apical compartment. Monolayers include control conditions (top), and after addition of amiloride (100 μM), ATP (100 μM), or amiloride and ATP together (bottom). Bar shown in bottom panel represents 10 μm. B. Cumulative data demonstrating effect of amiloride (n=8), ATP (n=8), or amiloride and ATP together (n=9) on ASL height compared to control monolayers (n=9), *p<0.05 versus control, **p<0.01 versus control, #p<0.05 versus amiloride alone.

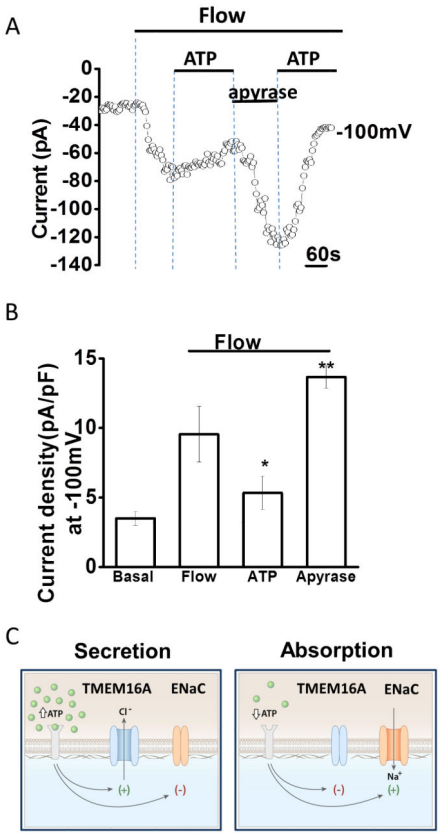

Figure 7. Flow-stimulated Na^+ currents are regulated by extracellular ATP

Whole-cell currents were measured during basal conditions and during exposure to flow (shear =0.24 dyne/cm^2) in the absence or presence of ATP (100 μM) or apyrase (5 unit/ml). A. Representative whole-cell recording with currents measured at −100 mV and at 100 mV shown. Flow exposure (shear of 0. 24 dyne/cm^2) is indicated by the top bar. Currents activated rapidly with the onset of flow and were partially inhibited when ATP was included in the perfusate as indicated by the lower line. Subsequent removal of ATP and addition of apyrase resulted in rapid activation of currents. Re-application of ATP inhibited currents. B. Cumulative data demonstrating maximal flow-stimulated current density in control conditions or in the presence of ATP, or apyrase. Values represent maximal current density measured at −100 mV (n=4-5 each), *p< 0.05 versus control, **p<0.01 versus control. C. Proposed model for the coordination of biliary epithelial secretion and absorption by extracellular ATP. According to this model, when the concentration of ATP in bile is high, TMEM16A is activated, ENaC is inhibited, and net secretion occurs. When the concentration of ATP in bile drops, TMEM16A inactivates, the inhibitory effect of ATP on ENaC is abolished, and net absorption occurs.